

SUPPORT CHEMISTRY, SURFACE AREA, AND PREPARATION EFFECTS ON SULFIDED NiMo CATALYST ACTIVITY

Timothy J. Gardner, Linda I. McLaughlin, and Ronald S. Sandoval
Sandia National Laboratories
Process Research Department, Mail Stop 0709
P.O. Box 5800
Albuquerque, NM 87185-0709

Keywords: oxide supports, hydrotreating catalysts, hydrous titanium oxide

INTRODUCTION

Hydrous Metal Oxides (HMOs) are chemically synthesized materials which contain a homogeneous distribution of ion exchangeable alkali cations that provide charge compensation to the metal-oxygen framework. In terms of the major types of inorganic ion exchangers defined by Clearfield,¹ these amorphous HMO materials are similar to both hydrous oxides and layered oxide ion exchangers (e.g., alkali metal titanates). For catalyst applications, the HMO material serves as an ion exchangeable support which facilitates the uniform incorporation of catalyst precursor species. Following catalyst precursor incorporation, an activation step is required to convert the catalyst precursor to the desired active phase.

Considerable process development activities at Sandia National Laboratories related to HMO materials have resulted in bulk hydrous titanium oxide (HTO)- and silica-doped hydrous titanium oxide (HTO:Si)-supported NiMo catalysts that are more active in model reactions which simulate direct coal liquefaction (e.g., pyrene hydrogenation) than commercial γ -Al₂O₃-supported NiMo catalysts.²⁻⁷ However, a fundamental explanation does not exist for the enhanced activity of these novel catalyst materials; possible reasons include fundamental differences in support chemistry relative to commercial oxides, high surface area, or catalyst preparation effects (ion exchange vs. incipient wetness impregnation techniques). The goals of this paper are to identify the key factors which control sulfided NiMo catalyst activity, including those characteristics of HTO- and HTO:Si-supported NiMo catalysts which uniquely set them apart from conventional oxide supports.

EXPERIMENTAL PROCEDURE

Support chemistry effects were examined using both commercially-available oxide supports and HTO/HTO:Si supports. Commercial oxide supports studied included γ -Al₂O₃ (in extrudate form, 1/16 in. diameter) and various commercial forms of TiO₂. In order to fairly evaluate the effect of support chemistry between the commercial oxide and HTO/HTO:Si supports, it was necessary to normalize the Mo loadings per unit surface area. This approach has been previously used with success to differentiate support chemistry effects for hydrodesulfurization reactions.⁸ Because it is well known that the surface area of oxide support materials can change significantly with processing (Mo loading, calcination, etc.), it was necessary to select a specific processing state to use as a reference point for catalyst support surface area. We used the support surface area after a standard calcination treatment in air at 500°C for 1 h as a reference point, since this would effectively represent the amount of support surface area available to disperse the molybdenum oxide phase which formed during the calcination procedure.

Table 1 shows the differences between the various supports evaluated in this study in terms of the method of preparation and their surface area, both as-received and after a standard calcination procedure. The surface area of the γ -Al₂O₃ extrudate is fairly typical of γ -Al₂O₃ catalyst supports, and was relatively unchanged after the calcination treatment. The titania supports exhibited different thermal stabilities depending on the preparation method, with the calcined surface area values correlating well with the crystallographic phase evolution of TiO₂. The Degussa P25 TiO₂, prepared by a high temperature flame hydrolysis procedure, showed only a slight decrease in surface area as a result of the calcination procedure. This moderate surface area material consisted of a mixture of anatase and rutile phases of TiO₂. The Ti oxide TiO₂ material is prepared via a precipitation process using sulfate precursors followed by low temperature heat treatment to produce a high surface area anatase material. Further heat treatment of this material via calcination

resulted in significant surface area reduction and partial conversion of anatase to rutile. The HTO and HTO:Si supports were evaluated in acidified form following complete H^+/Na^+ exchange. In their as-prepared forms, these materials exhibit very high surface areas ($\sim 400 \text{ m}^2/\text{g}$). These acidified forms are generally representative of the final HTO or HTO:Si support material which remains following ion exchange (IE) processing. Calcination of these as-prepared materials results in significant surface area reduction. However, SiO_2 additions to HTO materials act to stabilize support surface area at high temperature ($\geq 500^\circ\text{C}$) without significantly altering ion exchange properties.^{6,7,9} The improved thermal stability of the HTO:Si supports is due to the retardation of the anatase to rutile phase transformation by the SiO_2 dopant, which has been extensively documented in the literature.¹⁰⁻¹³

Table 1
Oxide Support Characteristics

Support Material	Preparation Technique	As-Received Surface Area (m^2/g)	Calcined Surface Area (m^2/g)*
Degussa P25 TiO_2	Flame Hydrolysis	52	47
Tioxide TiO_2	Precipitation	183	120
H^+ /HTO	Sol-Gel + IE	417	63
H^+ /HTO:Si	Sol-Gel + IE	390	184
$\gamma\text{-Al}_2\text{O}_3$ Extrudate	Precipitation + Extrusion	235	227

* Calcination procedure: $500^\circ\text{C}/1\text{h}/\text{air}$. Surface area was measured by the BET method.

HTO and HTO:Si ion exchangeable supports (Na:Ti and Si:Ti molar ratios = 0.5 and 0.2, respectively) were fabricated using the standard multiple step sol-gel chemistry procedure which has been described in detail elsewhere.^{3,8,7,14} HTO- and HTO:Si-supported NiMo catalyst preparation was performed using a two step procedure featuring Mo anion ($[\text{Mo}_7\text{O}_{24}]^{6-}$) exchange/adsorption followed by incipient wetness impregnation using $\text{Ni}(\text{NO}_3)_2 \cdot 6\text{H}_2\text{O}$. For the commercial oxide-supported NiMo catalysts, only incipient wetness impregnation techniques were used; two separate impregnation steps were used, first with ammonium heptamolybdate ($(\text{NH}_4)_6\text{Mo}_7\text{O}_{24} \cdot 4\text{H}_2\text{O}$), and next with nickel nitrate ($\text{Ni}(\text{NO}_3)_2 \cdot 6\text{H}_2\text{O}$) precursors. Supported Mo and NiMo catalysts with Mo loadings ranging from 0.6 to 25 Mo atoms/ nm^2 support surface area were fabricated as part of this study. This range of Mo loadings corresponded to a wide overall range of Mo weight loadings, 0.1 to 25 wt. % (calcined basis), on the various supports. Regardless of the Mo loading level in the catalyst, a constant ratio of moles Ni/(moles Ni + moles Mo) = 0.35 was used to determine the Ni loading for each supported NiMo catalyst.

The final catalyst precursors were activated by first calcining in air at 500°C for 1 h and then sulfiding in 10% H_2S in H_2 at 420°C for 2 h. All TiO_2 (including HTO and HTO:Si)-supported catalysts were pelletized and granulated to -10/+20 mesh prior to activation, and all catalysts were ground and sieved to -200 mesh prior to testing. Catalyst activity was evaluated using two different model reactions representative of hydrotreating reactions: pyrene hydrogenation and dibenzothiophene hydrodesulfurization. For the pyrene hydrogenation tests, pyrene (0.1 g), hexadecane (1 g), and catalyst (0.010 g) were loaded into a batch microautoclave reactor and tested at 300°C under 500 psig H_2 for 10 min. For the dibenzothiophene hydrodesulfurization tests, dibenzothiophene (0.1 g), hexadecane (1 g), and catalyst (0.050 g) were loaded into a batch microautoclave reactor and tested at 350°C under 1200 psig H_2 for 10 min. Reversible first-order kinetics were used to model the pyrene hydrogenation test results,¹⁵ while irreversible first-order kinetics were used to model the dibenzothiophene hydrodesulfurization test results.¹⁶

RESULTS AND DISCUSSION

Figure 1 summarizes the catalyst activity trends observed for the pyrene hydrogenation testing of the sulfided NiMo catalysts. This type of figure, plotting the intrinsic pyrene hydrogenation activity (rate per g total active metal [Ni+Mo]) vs. specific Mo loading (in Mo atoms/ nm^2 calcined support surface area) is used to

normalize surface area differences among the various supports examined in this study. For NiMo/ γ -Al₂O₃ catalysts, the intrinsic pyrene hydrogenation activity is stable at low specific Mo loadings, but decreases with increasing specific Mo loading. This behavior is in contrast to that observed for TiO₂-supported catalysts (including HTO and HTO:Si supports), where we find that a maximum in intrinsic pyrene hydrogenation activity is observed as specific Mo loading is increased. Very similar trends, including the location and value of the maximum in the intrinsic pyrene hydrogenation activity, were observed for all of the commercial TiO₂ materials evaluated: Degussa P25 TiO₂, Tioxide TiO₂, and a low surface area (10 m²/g) rutile form of TiO₂. The characteristic behavior of sulfided NiMo catalysts supported on these commercial TiO₂ support materials is illustrated in Figure 1 by the data shown for the Degussa P25 TiO₂-supported NiMo catalysts.

However, as shown in Figure 1, the location of the maximum in the intrinsic pyrene hydrogenation activity is different for the commercial TiO₂ supports with respect to the HTO or HTO:Si supports. Since the data shown in Figure 1 has been normalized to remove support surface area effects, the differences in behavior for the HTO and HTO:Si supports must be attributable to other fundamental differences in support chemistry or catalyst preparation effects. The HTO-supported NiMo catalysts show a broad range of relatively high activity with the maximum in activity shifted to higher specific Mo loadings. This behavior shows a distinct advantage over typical commercial catalysts since it accommodates higher overall catalyst activities at high weight loading. The controlled addition of SiO₂ to the HTO support produces significant changes in this behavior. The peak intrinsic pyrene hydrogenation activity shifts to very low specific Mo loadings (lower than those observed for the commercial titanias) and is significantly increased in magnitude. This result indicates an important role of the SiO₂ dopant, which might be well dispersed on the surface of small anatase crystallites, therefore affecting the dispersion of the catalytic doped MoS₂ phase.

Similar trends to those shown in Figure 1 were also observed for Mo only catalysts, although intrinsic pyrene hydrogenation activities were consistently lower. It should be noted that due to the limited number of data points for some of the curves in Figure 1 (e.g., Degussa P25 TiO₂ and γ -Al₂O₃ supports), we can only speculate on the presence and/or location of the maximum in catalyst activity. Obviously, more data is necessary to make firm conclusions with respect to these trends.

Similar studies have been performed using the dibenzothiophene hydrodesulfurization model reaction. Very different trends are observed for this model compound reaction in terms of the intrinsic catalyst activity vs. specific Mo loading. Thus far, a valid comparison has been made only with the γ -Al₂O₃, TiO₂, and HTO-supported Mo catalysts. These results are shown in Figure 2. In one case (P25 TiO₂ support), both Mo- and NiMo-supported catalysts have been tested. As shown in Figure 2, and consistent with a vast quantity of published literature, the addition of Ni results in a significant promotional effect for the dibenzothiophene hydrodesulfurization reaction.^{17,18} However, the trends for TiO₂-supported catalysts are very different for dibenzothiophene hydrodesulfurization compared to pyrene hydrogenation (see Figure 1). All TiO₂-supported catalysts examined to date (including HTO supports) exhibit very high intrinsic activity for dibenzothiophene hydrodesulfurization at low specific Mo loadings, with activity sharply decreasing as Mo loading is increased. In contrast to this behavior, γ -Al₂O₃-supported catalysts exhibit behavior very similar to that observed for pyrene hydrogenation. These trends observed for dibenzothiophene hydrodesulfurization with the TiO₂ (including HTO)- and γ -Al₂O₃-supported Mo catalysts are consistent with those observed previously for thiophene hydrodesulfurization.⁸ The fact that the intrinsic activity for all of the TiO₂-supported catalysts is higher than that observed for the γ -Al₂O₃-supported catalysts is also consistent with previous work.⁸

These early results indicate that different types of catalysts, in terms of Mo loading, are optimum for hydrogenation vs. hydrodesulfurization reactions. This is consistent with evidence published in the literature suggesting that hydrogenation and hydrodesulfurization reactions take place on different types of active sites.^{19,20} These results also show that the HTO-or HTO:Si-based supports may offer more significant advantages for hydrogenation rather than hydrodesulfurization applications.

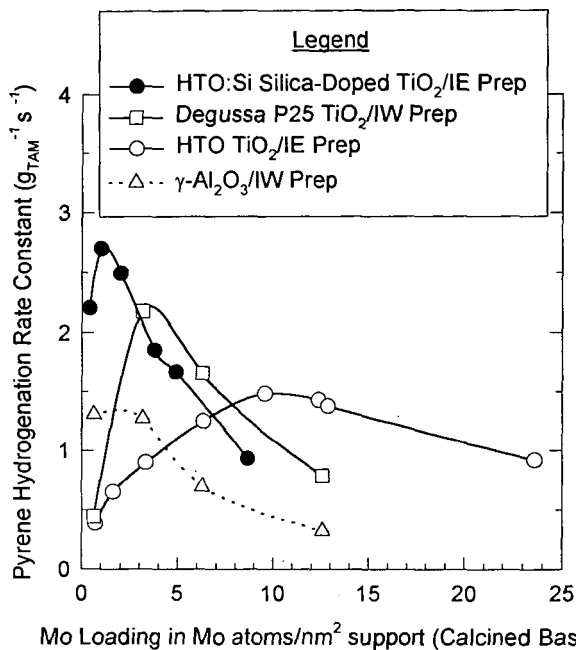


Figure 1. Intrinsic pyrene hydrogenation activity (rate per g total active metal) vs. specific Mo loading (in Mo/nm² support) for sulfided NiMo catalysts supported on various oxide supports. The acronyms IW and IE in the legend correspond to incipient wetness impregnation and ion exchange preparation techniques, respectively.

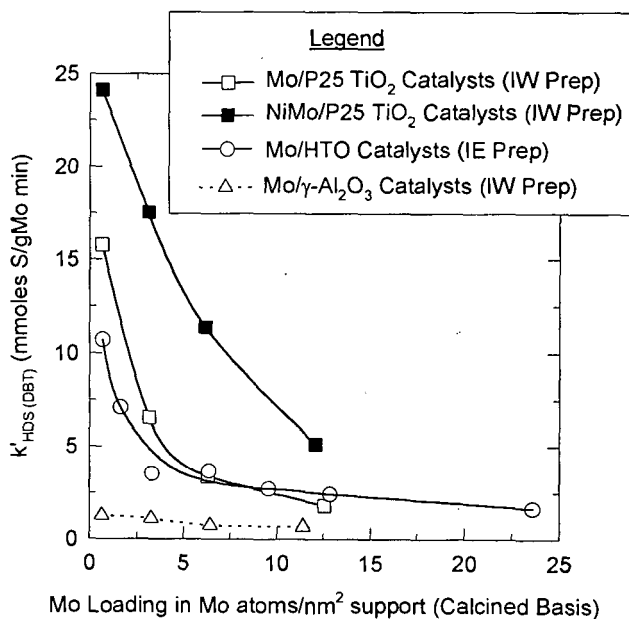


Figure 2. Intrinsic dibenzothiophene hydrodesulfurization activity results vs. specific Mo loading (in Mo atoms/nm² support) for selected sulfided Mo- and NiMo-based catalysts. Note that the acronyms shown in the legend were previously defined in the caption for Figure 1.

Additional work is necessary to further investigate the interesting behavior and potential benefits of the HTO- and HTO:Si-based supports. This work will include assessments of changes in MoS₂ dispersion as a function of Mo loading and support chemistry.

SUMMARY

This work has evaluated various catalyst support chemistries with a range of Mo loadings (normalized with respect to surface area) for both pyrene hydrogenation and dibenzothiophene hydrodesulfurization reactions. γ -Al₂O₃-supported Mo and NiMo catalysts were found to behave similarly with respect to both model reactions; intrinsic catalyst activity was relatively constant at low Mo loadings, but slightly decreased with increasing Mo loading. Significant differences were observed for the TiO₂ supports evaluated in this study, both with respect to the γ -Al₂O₃-supported catalyst results and for the different types of TiO₂ supports (including the HTO and HTO:Si materials). For pyrene hydrogenation, all TiO₂-supported catalysts showed a maximum in intrinsic catalyst activity, with the position of the maximum varying with changes in support chemistry and catalyst preparation procedures. In contrast to the pyrene hydrogenation results, all TiO₂-supported Mo catalysts showed a similar trend of significantly decreasing intrinsic catalyst activity with increasing Mo loading for the dibenzothiophene hydrodesulfurization model reaction. These results therefore indicate that HTO-based supports may offer more significant advantages for hydrogenation rather than hydrodesulfurization applications. Experiments are in progress to evaluate changes in MoS₂ dispersion as a function of support chemistry and Mo loading.

This work was performed at Sandia National Laboratories and was supported by the U.S. Department of Energy under contract DE-AC04-94AL85000.

REFERENCES

1. A. Clearfield, Ind. Eng. Chem. Res. **34**, 2865 (1995).
2. H. P. Stephens, R. G. Dosch, and F. V. Stohl, Ind. Eng. Chem. Res. Devel. **24**, 15 (1985).
3. H. P. Stephens and R. G. Dosch, Stud. Surf. Sci. Catal. **31**, 271 (1987).
4. S. E. Lott, T. J. Gardner, L. I. McLaughlin, and J. B. Oelfke, Submitted to Fuel.
5. S. E. Lott, T. J. Gardner, L. I. McLaughlin, and J. B. Oelfke, Prep. of Papers, Fuel Div., Amer. Chem. Soc. **39** 1073 (1994).
6. R. G. Dosch, H. P. Stephens, and F. V. Stohl, Sandia Report, SAND89-2400, Sandia National Laboratories, Albuquerque, NM, 1990.
7. R. G. Dosch and L. I. McLaughlin, Sandia Report, SAND92-0388, Sandia National Laboratories, Albuquerque, NM, 1992.
8. K. C. Pratt, J. V. Sanders, and V. Christov, J. Catal. **124**, 416 (1990).
9. T. J. Gardner and L. I. McLaughlin, Submitted to Mater. Res. Soc. Symp. Proc.
10. Y. Suyama and A. Kato, Yogyo-Kyokai-Shi **86**(3), 119 (1978).
11. C. U. I. Odenbrand, S. L. T. Andersson, L. A. H. Andersson, J. G. M. Brandin, and G. Busca, J. Catal. **125**, 541 (1990).
12. J. R. Sohn, H. J. Jang, M. Y. Park, E. H. Park, and S. E. Park, J. Mol. Catal. **93**, 149 (1994).
13. P. K. Doolin, S. Alerasool, D. J. Zalewski, and J. F. Hoffman, Catal. Lett. **25**, 209 (1994).
14. R. G. Dosch, H. P. Stephens, F. V. Stohl, B. C. Bunker, and C. H. F. Peden, Sandia Report, SAND89-2399, Sandia National Laboratories, Albuquerque, NM, 1990.
15. H. P. Stephens and R. J. Kottenstette, Prep. of Papers, Fuel Div., Amer. Chem. Soc. **30**, 345 (1985).
16. O. Weisser and S. Landa, Sulfide Catalysts, Their Properties and Applications, Pergamon Press, Oxford, 1973.
17. R. R. Chianelli, M. Daage, and M. J. Ledoux, Adv. Catal. **40**, 177 (1994).
18. M. J. Ledoux, S. Hantzer, and J. Guille, Bull. Soc. Chim. Belg. **96**(11-12), 855 (1987).
19. A. Stanislaus and B. H. Cooper, Catal. Rev.-Sci. Eng. **36**(1), 75 (1994).
20. M. Daage and R. R. Chianelli, J. Catal. **149**, 414 (1994).